

Surface effects on core-level binding energies and valence in thulium chalcogenides

G. Kaindl and C. Laubschat

*Institut für Atom- und Festkörperphysik, Freie Universität Berlin, D-1000 Berlin 33, Germany*B. Reihl, R. A. Pollak, N. Mårtensson, F. Holtzberg, and D. E. Eastman
IBM Thomas J. Watson Research Center, Yorktown Heights, New York 10598

(Received 18 January 1982)

Vacuum-cleaved (100) surfaces of mixed-valent TmSe, divalent TmTe, and trivalent TmS were studied by high-resolution, angle-integrated photoelectron spectroscopy with the use of synchrotron radiation in the energy range $30 \leq h\nu \leq 110$ eV. In the topmost surface layers of TmSe and TmTe the 4*f* levels are found to be shifted to higher binding energies by 0.32 ± 0.04 and 0.41 ± 0.05 eV, respectively. In both TmSe and TmS the topmost surface layers are divalent. In the case of TmSe a separation of the $Tm^{2+} 4f^{12}$ spectral feature into surface and bulk contributions allows a determination of the bulk mean valence $\bar{v} = 2.55 \pm 0.05$. While a shift of the Se 3*d* levels to lower binding energy is observed for Se atoms in the topmost surface layer of TmSe, no such shift can be resolved for the Te 4*d* levels of TmTe. The surface-derived divalent spectral features can be quenched completely in all three cases by exposure of the surfaces to submonolayer amounts of oxygen, resulting in the formation of trivalent surface oxides. Values for the electron mean free path *l* are derived from the observed surface- and bulk-spectral intensities, with *l* decreasing with decreasing electron kinetic energy down to $\cong 45$ eV. Smaller singularity indices α of the Doniach-Sunjić line shapes as well as smaller extrinsic losses are observed for photoemission from the divalent surface layers as compared to the bulk.

I. INTRODUCTION

Recent photoemission studies of rare-earth solids have revealed in a number of cases surface-induced changes of both the mean valence of the rare-earth ion and of the 4*f* binding energies. Theoretically, these effects may be understood as a consequence of the decrease in cohesive energy due to reduced coordination when a rare-earth ion is brought from the bulk to the surface.¹⁻³ A surface valence transition was first observed for bulk trivalent Sm metal,⁴⁻⁶ where it was shown that the outermost surface layer of Sm is essentially divalent. Later on, surface valence transitions have also been observed for YbAu₂ (Refs. 7 and 8) and amorphous SmAu alloys.⁹ Quite recently it was shown that in mixed-valent YbAl₂ more than one surface layer is involved in a valence transition to the divalent or almost divalent state,¹⁰ giving rise to predominantly divalent features in the uv-photoemission spectra. This observation has subsequently been confirmed for other intermediate-valent rare-earth systems.^{11,12}

Surface effects on core-level binding energies, which had originally been found for 5*d* transition metals,¹³⁻¹⁵ have recently also been reported for quite a few rare-earth metals.¹⁶⁻²¹ Such surface

core-level shifts could also be observed for stable-valent rare-earth chalcogenides, such as SmS, SmSe,^{22,23} EuS, YbS,²³ several intermetallic compounds,²⁴ and the mixed-valent systems SmB₆,¹⁸ CeN,²² YbAl₂,¹⁰ EuPd₂Si₂,¹² and Sm_{1-x}Y_xS.¹¹ In all cases the 4*f* levels were found to be shifted to higher binding energy at the surface, in agreement with theoretical prediction.¹ No surface effects on valence or 4*f* binding energy, however, have been reported up to now for Tm systems.²⁵

The aim of the present work was therefore mainly concerned with a systematic study of surface effects on valence and 4*f* binding energy in Tm systems, especially the Tm monochalcogenides, TmX, with X = S, Se, Te. This series of isostructural compounds (NaCl structure) was chosen because of their remarkably different physical properties, and the ease with which well-defined clean crystal faces may be prepared by cleaving in UHV. Metallic TmS is now considered to be trivalent, TmTe is divalent and behaves like a semiconductor, while TmSe is homogeneously mixed valent.^{26,27} The Tm monochalcogenides, including mixed-valent TmSe, order antiferromagnetically at low temperatures.^{26,28,29} Valence and lattice constant of Tm_xSe are known to vary appreciably with stoichiometry.^{28,30-32} The exact value of the bulk

mean valence of stoichiometric TmSe ($a_0 \cong 5.71 \text{ \AA}$) has been subject to some controversy, since from lattice constant systematics $\bar{v} \cong 2.75$ was derived,^{28,30} while x-ray photoemission spectroscopy (XPS) studies,³¹ x-ray-absorption *L*-edge measurements,^{33,34} and magnetic measurements^{28,30} resulted in $\bar{v} = 2.55$ to 2.60.

The paper is arranged as follows: After some experimental remarks in the following section, the experimental results including details of the data analysis will be presented in Sec. III for the three single-crystalline compounds studied. In Sec. IV the results concerning the observed surface core-level shifts in TmSe and TmTe as well as the surface valence transitions in TmSe and TmS are discussed. In addition, values for the electron mean free path l are derived as a function of the electron kinetic energy for the three compounds studied, and the observed intensities of the individual lines of the $4f$ final-state multiplets of Tm^{2+} and Tm^{3+} are compared with the results of theoretical calculations.^{35,36}

II. EXPERIMENTAL DETAILS

The photoemission experiments were performed at the Synchrotron-Radiation Center of the University of Wisconsin—Madison, using a display-type photoelectron spectrometer and a toroidal-grating monochromator for photon energies $5 \leq h\nu \leq 130 \text{ eV}$.³⁷ The spectrometer was operated in the angle-integrated mode with electrons accepted within a 35° cone with axis normal to the surfaces of the samples. The combined system of spectrometer and monochromator gave a resolution of about 0.17 eV for $h\nu = 70 \text{ eV}$ as determined from the width of Fermi edges.

All samples of Tm chalcogenides studied were in the form of single crystals, which had been prepared by a method described previously.³⁸ The UHV conditions of the spectrometer (1×10^{-10} Torr in the preparation chamber and 4×10^{-11} Torr in the main spectrometer chamber) together with the favorable intensity of the system allowed spectra to be taken on very clean surfaces. Spectra covering an energy range of 15 eV were typically recorded within 7 min. All measurements were performed at room temperature on the (100) surfaces cleaved in vacuum, typically within 10–90 min after a cleave. With the samples in the main spectrometer chamber (4×10^{-11} Torr), no changes in the spectral features were detected within a period of up to 2 h after a cleave.

III. EXPERIMENTAL RESULTS AND DATA ANALYSIS

A. TmSe (100)

The photoemission spectra obtained from the (100) surface of mixed-valent TmSe are shown in Fig. 1. The valence-band spectra of the freshly cleaved surface are dominated by emission from the localized $4f$ states of the Tm ion at the three photon energies employed [Fig. 1(a), 45 eV; Fig. 1(b), 70 eV; Fig. 1(c), 100 eV]. Since TmSe is known to be a homogeneously mixed-valent material, the ground state of the Tm ion is a mixture of two energetically degenerate configurations with different $4f$ occupations, namely the trivalent $\text{Tm } 4f^{12}5d^1$ and the divalent $\text{Tm } 4f^{13}5d^0$ configurations. Photoemission from the $4f$ states therefore leads to characteristic multiplet spectra of the $4f^{11}$ and $4f^{12}$ final states, which are energetically separated by the Coulomb correlation energy U , amounting to about 6 eV for the Tm ion.^{31,39}

The relative energetic positions of the individual components of the $4f^{12}$ final-state multiplet are expected to be well represented by the excited states of trivalent Tm as obtained from uv-absorption measurements.⁴⁰ The $4f^{11}$ final-state multiplet spectrum of trivalent Tm, however, has to be compared with the excited states of trivalent Er, since—due to the instability of Tm^{4+} —no optical-absorption data exist for this ion. Since the effective nuclear charge for the $4f$ shell is larger by one unit for Tm as compared to Er, the separation of the $4f^{11}$ -multiplet lines should be larger for the Tm ion as compared to Er. The intensities of the multiplet lines were taken from the results of fractional-parentage calculations, assuming *LS* coupling,³⁵ or from improved intermediate-coupling calculations available for the $4f^{12}$ multiplet³⁶ and for a few components of the $4f^{11}$ multiplet.⁴¹ For some multiplet lines, empirical adjustments were made to the theoretical intensities in order to reach optimum least-squares fits of the spectra (see below and Table I).

The solid bar diagrams in Fig. 1(b) represent the relative positions and intensities of the two final-state multiplets. It is obvious from an inspection of Figs. 1(a) and 1(b) that the $4f^{12}$ part of the spectrum cannot be described by a single $4f^{12}$ final-state multiplet alone. Instead, it is a superposition of two $4f^{12}$ multiplets, shifted by about 0.3 eV. The dotted multiplet, shifted to higher binding energy, is interpreted as originating from Tm^{2+} ions in the topmost surface layer, while the

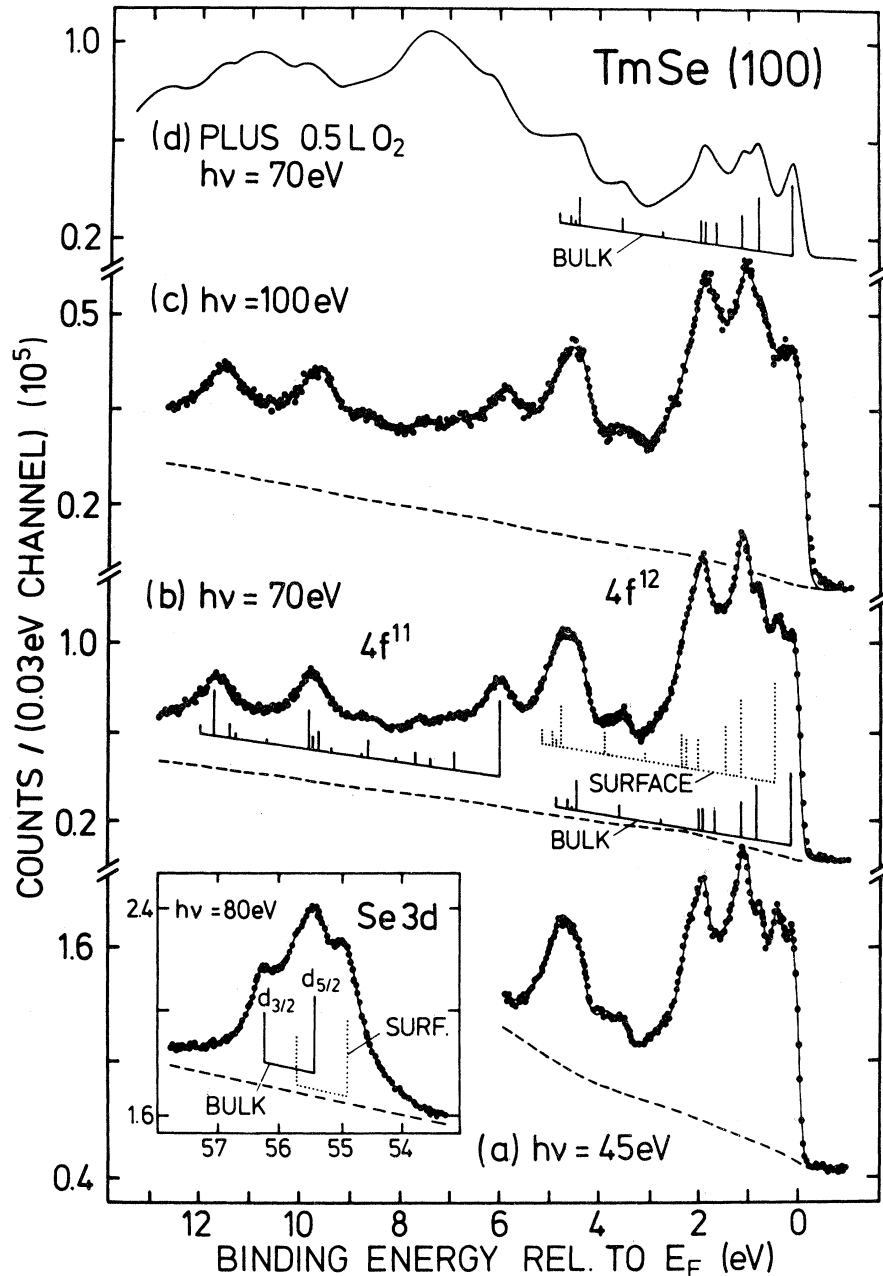


FIG. 1. Photoemission spectra of the (100) surface of TmSe excited with photons of the given energies: (a)–(c) freshly cleaved, and (d) after exposure to 0.5 L of oxygen. The bar diagrams represent the positions and relative intensities of the final-state $4f$ -multiplet components originating from the bulk (solid bars) and from a surface layer (dotted bars). The spectrum obtained of the Se $3d$ core levels is given in the inset. The solid lines in (a)–(c) and in the inset represent the results of least-squares fits (see text), with the resulting integral background plotted separately as a dashed line.

solid multiplet corresponds to emission from the bulk. This surface core-level shift is most clearly visible in the splitting of the first multiplet line just below the Fermi level [see Figs. 1(a) and 1(b)].

The correctness of the above assignment of the

$4f^{12}$ multiplet with higher binding energy as surface emission was tested by exposure of the TmSe(100) surface to 0.5 and 1.5 L of oxygen. The spectrum obtained with 70-eV photons after exposure to 0.5 L of O_2 is shown in Fig. 1(d).

TABLE I. Energies and relative intensities of the $4f^{12}$ (Tm^{2+}) and $4f^{11}$ (Tm^{3+}) final-state multiplets employed in the TmSe fits.

Final state	Tm^{2+}		Final state	Tm^{3+}	
	Energy (eV)	Intensity		Energy ^a (eV)	Intensity
3H_6	0	2.90 ^b	$^4I_{15/2}$	0	2.54
3F_4	0.695	2.20 ^b	$^4I_{13/2}$	0.805	0.60 ^c
3H_5	1.015	1.38	$^4I_{11/2}$	1.253	0.21
3H_4	1.552	0.90 ^b	$^4I_{9/2}$	1.521	0.40 ^c
3F_3	1.774	0.88	$^4F_{9/2}$	1.877	0.15 ^c
3F_2	1.849	0.90 ^b	$^2H_{11/2}$	2.374	0.60 ^c
1G_4	2.625	0.22	$^4F_{7/2}$	2.518	0.15
1D_2	3.450	0.60 ^b	$^2G_{9/2}$	3.025	0.20 ^c
1I_6	4.300	1.20 ^b	$^4G_{11/2}$	3.271	0.64 ^c
3P_0	4.393	0.16	$^4G_{9/2}$	3.393	0.42
3P_1	4.475	0.38	$^2K_{15/2}$	3.433	1.29
3P_2	4.710	0.36	$^4G_{7/2}$	4.205	0.11
1S_0	9.843	0.09	$^2D_{5/2}$	4.769	0.15 ^c
			$^4D_{7/2}$	4.841	0.40 ^c
			$^2L_{17/2}$	5.155	1.50
			$^2I_{13/2}$	5.407	0.24

^aThese energies are for the $4f^{11}$ multiplet of Er^{3+} (Ref. 40). To fit the experimental spectra of Tm^{3+} they had to be multiplied by a factor of 1.11.

^bAdjusted intensities deviate from the theoretical ones of Ref. 36 (intermediate coupling).

^cAdjusted intensities deviate from the theoretical ones of Refs. 35 and 41 (mostly *LS* coupling).

When compared with the 70-eV spectrum of the clean surface [Fig. 1(b)] it is obvious that the $4f^{12}$ surface multiplet is almost completely quenched in the spectrum of Fig. 1(d). Therefore, the spectral features in the $4f^{12}$ region are well described by the single $4f^{12}$ bulk multiplet indicated by the solid bar diagram. The exposure to oxygen causes an additional $4f^{11}$ final-state feature in the spectrum of Fig. 1(d), which is shifted by about 1.3 eV to higher binding energy relative to the $4f^{11}$ feature in the spectrum of clean TmSe(100). This oxygen-induced $4f^{11}$ feature originates from a trivalent surface layer such as e.g., $(\text{TmO})_2\text{Se}$.⁴² The reduced metallic screening of the final-state core hole in such an insulating surface layer would explain the observed higher binding energy. After exposure to 1.5 L of O_2 the $4f^{12}$ feature in the spectrum (not shown here) sharpens up even more with the most intense feature then being the $4f^{11}$ multiplet from the trivalent oxygen compound, which extends now over more than one surface layer.

The spectra in Figs. 1(a)–1(c) were least-squares fitted to a superposition of two $4f^{12}$ multiplets (bulk and surface) and one $4f^{11}$ multiplet with relative energies and intensities as given in Table I. Doniach-Šunjić line shapes⁴³ with linewidth γ and

the singularity index α as parameters were used, and the resulting lines were folded with a Gaussian approximating the instrumental resolution (monochromator and spectrometer). Above the Fermi edge all Doniach-Šunjić lines were abruptly set to zero. The use of Doniach-Šunjić lines takes intrinsic losses due to excitations in the conduction band during the photoemission process into account. In addition, a background of scattered electrons proportional to the integrated photoemission above a given energy was added to the theoretical spectrum, taking care of extrinsic energy losses of photoelectrons on their way through the solid. Two different proportionality constants had to be employed as fit parameters of the backgrounds created by emission from bulk and surface layers in order to get satisfactory results. The fits gave consistently smaller extrinsic background parameters for emission from the surface layer as compared to the bulk, in agreement with expectation. In addition, a Gaussian with fixed position (at 7.5-eV binding energy relative to E_F) and fixed width [5-eV full width at half-maximum (FWHM)] but variable intensity was added to the spectrum to describe the relatively weak emission from Se $4p$ levels. Position and width of this line were taken from an uv-photoemission measurement of TmSe

at $h\nu=21.2$ eV,⁴⁴ where it appeared dominant in the spectrum due to the strongly reduced cross section for emission from $4f$ states.⁴⁵ Only at $h\nu=45$ eV did the fits show a noticeable intensity for the Se $4p$ line, which was added in Fig. 1(a) to the extrinsic background (dashed line).

The results of the least-squares-fit analysis are represented in Figs. 1(a)–1(c) by the solid lines, and it is obvious that the agreement between fitted curves and measured data points is rather good. The energies (relative to the multiplet line with lowest binding energy) and the relative intensities of the individual components of the $4f^{12}$ (Tm^{2+}) and $4f^{11}$ (Tm^{3+}) final-state multiplets employed in the least-squares fits of the spectra of Figs. 1(a)–1(c) are tabulated in Table I. In order to fit the experimental data, the intensities of several lines of both multiplets (indicated in Table I) had to be changed as compared to the theoretical values.

The results of the least-squares fits of the spectra in Figs. 1(a)–1(c) are summarized in Table II. For both the $4f^{11}$ and the $4f^{12}$ bulk multiplet, the singularity index was found to be $\alpha_B=0.17\pm 0.03$, while a reduced value of $\alpha_S=0.10\pm 0.05$ was adjusted to the surface multiplet. The linewidth parameters of the Doniach-Šunjić lines used to describe the three multiplets were $2\gamma_B^{12}=0.24$ eV, $2\gamma_S^{12}=0.40$ eV for the two $4f^{12}$ multiplets, and $2\gamma^{11}=0.68$ eV for the $4f^{11}$ multiplet. A mean value of $\Delta_c=0.32\pm 0.04$ eV is obtained for the surface core-level shift (column 2 of Table II), and the binding-energy difference between the lowest binding-energy multiplet lines of the $4f^{11}$ and $4f^{12}$ multiplets is found to be 5.91 ± 0.02 eV (columns 3 and 4 of Table II). The fractional intensities of the three multiplets are given in columns 5, 6, and 7 for the two photon energies (100 and 70 eV), for which complete valence-band photoemission spectra were recorded.

The inset in Fig. 1 shows the photoemission spectrum of the Se $3d$ core levels in $\text{TmSe}(100)$ recorded with a photon energy of 80 eV. Instead of a doublet of lines split by the spin-orbit splitting of the $3d_{3/2}$ and $3d_{5/2}$ hole states [$\Delta E_{so}=0.83$ eV in crystalline Se (Ref. 46)], a complex structure is observed, which could be fitted very well with a superposition of two doublets separated by $\Delta_c=0.52\pm 0.05$ eV. Again Doniach-Šunjić line shapes, folded with a Gaussian for the instrumental resolution, were used and the intensity ratio of the two lines in each doublet was set equal to the theoretical one [$I(d_{3/2})/I(d_{5/2})=\frac{2}{3}$]. The solid line represents the result of the least-squares fit. We interpret the doublet at lower binding energy as originating from the topmost surface layer. This assignment is supported by the fact that the surface doublet is suppressed in the spectrum taken from a $\text{TmSe}(100)$ surface exposed to 1.5 L of oxygen.

B. $\text{TmTe}(100)$

Similar measurements were performed on the (100) surface of TmTe , which is a divalent semiconductor. Valence-band spectra were recorded at photon energies of 50, 70, 90, and 110 eV of the freshly cleaved surface, and with 70- and 110-eV photons of a (100) surface exposed to 0.5 L of O_2 . Some representative spectra are displayed in Fig. 2 together with the results of least-squares fits. In addition, a photoemission spectrum of the Te $4d$ levels—shown in the inset—was recorded with 80-eV photons of a freshly cleaved surface.

The valence-band spectra of TmTe at photon energies $h\nu \geq 50$ eV are dominated by $4f$ emission from $4f^{12}$ (Tm^{2+}) final-state multiplets. In contrast to earlier XPS results,⁴⁷ which were most probably achieved on adsorbate-covered surfaces, the present spectra of freshly cleaved TmTe surfaces are characterized by only very weak $4f^{11}$

TABLE II. Summary of results from the analysis of the TmSe spectra taken at three different photon energies: Δ_c is the surface core-level shift of the $4f^{12}$ multiplet, E is the binding energy of the multiplet component closest to E_F , and I represents the fractional integrated intensities of the two $4f^{12}$ (bulk and surface) and the $4f^{11}$ multiplet, respectively. Estimated error bars are given in parentheses in units of the last digit. Derived values for the bulk mean valence \bar{v} and the electron mean free path l (see Sec. IV) are listed in the last two columns.

$h\nu$ (eV)	Δ_c (eV)	E_B^{12} (eV)	E_B^{11} (eV)	I_B^{12}	I_S^{12}	I^{11}	\bar{v}	l (Å)
100	0.30 (6)	0.14 (3)	6.06 (5)	0.32 (2)	0.31 (2)	0.37	2.56 (6)	8.0 (10)
70	0.33 (5)	0.12 (3)	6.03 (5)	0.30 (2)	0.38 (2)	0.32	2.53 (6)	6.2 (10)
45	0.31 (5)	0.13 (3)						

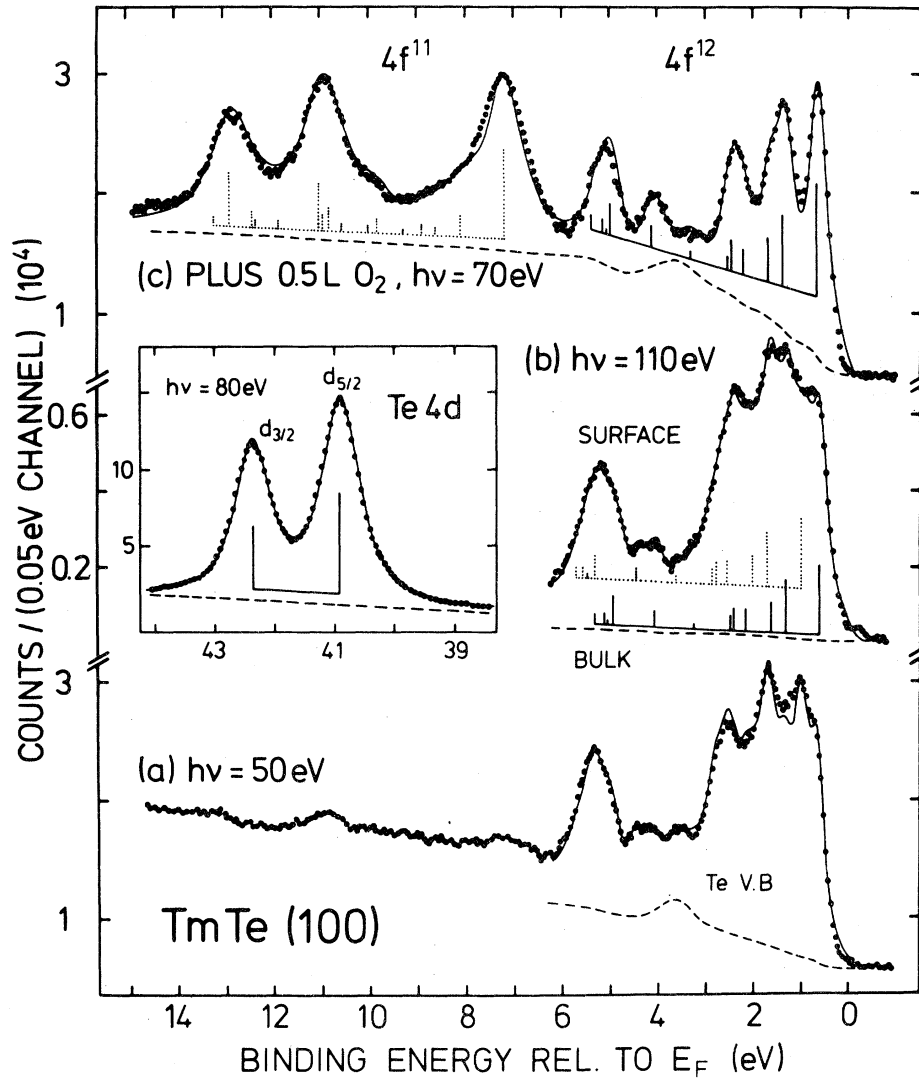


FIG. 2. Photoemission spectra of TmTe(100) obtained with various photon energies: (a) and (b) freshly cleaved, and (c) after exposure to 0.5 L of oxygen. The bar diagrams represent the final-state $4f$ multiplets from the bulk (solid bars) and from a surface layer (dotted bars). In the inset the spectrum of the Te $4d$ levels is given. The solid lines represent the results of least-squares fits (see text), and the dashed lines give the integral background plus the contributions from the Te valence band.

final-state multiplet lines [see Fig. 2(a)]. Since the sensitivity of the TmTe surface to adsorbates was previously demonstrated,⁴⁸ the weak spectral features seen in the $4f^{11}$ region of the present spectra are probably due to some trivalent surface contamination. The intensities of the $4f^{11}$ lines, however, did not noticeably change in the present experiments within a period of 2 h after cleaving in a vacuum of 4×10^{-11} Torr. Therefore, final-state effects cannot be ruled out completely as a possible cause.^{20,49}

The complicated structure of the $4f^{12}$ features of

the spectra of freshly cleaved TmTe(100) reveals the presence of a surface-shifted $4f^{12}$ multiplet as in the TmSe case. This was again proven by exposure of the surface to 0.5 L of O_2 [Fig. 2(c)], whereby the surface-derived multiplet was completely quenched. The $4f^{12}$ part of the spectrum of Fig. 2(c) can therefore be well described by a single $4f^{12}$ multiplet. In addition, an intense $4f^{11}$ -multiplet structure is recorded arising from an oxygen-compound surface layer, most probably $(TmO)_2Te$.⁴²

The spectra were least-squares fitted with a simi-

lar procedure as described in the TmSe case. To take into account emission from the Te-derived valence-band levels, two Gaussians of fixed positions (3.65 and 5.25 eV to E_F) and fixed widths (1.15 and 1.0 eV FWHM, respectively), but variable amplitudes, were added to the $4f^{12}$ -derived multiplet of Doniach-Šunjić-shaped lines. The positions and widths of these Te-derived peaks were taken from Ref. 48. In order to obtain optimum fits, the intensities of three $4f^{12}$ -multiplet lines had to be slightly changed from the numbers used in the TmSe fits (see Table I): 3H_5 was decreased to 1.20, 3F_2 was decreased to 0.50, and 1I_6 was decreased to 1.00. The results of the least-squares fits are again represented by the solid lines in Fig. 2 and summarized in Table III. From the surface core-level shifts listed in column 2 of Table III a mean value of $\Delta_c = 0.41 \pm 0.05$ eV is obtained for TmTe(100). The binding energy of the bulk $4f^{12}$ -multiplet line with lowest binding energy is found to be $E_B^{12} = 0.65$ eV relative to E_F , which clearly shows that TmTe cannot be a homogeneous mixed-valent material. The position of the $4f^{12}$ multiplet is in agreement with the results of Ref. 48 and supports the concept of TmTe being a divalent semiconductor. The binding energy of the uppermost $4f^{11}$ -multiplet line of the spectrum of Fig. 1(c) is found to be 7.2 eV, which is very close to the equivalent binding energy in the spectrum of the oxygen-exposed TmSe(100) surface. This indicates the similar character of the O_2 -induced surface compounds in these two cases. In agreement with the TmSe results, the ratio R_1 of intensities of the $4f^{12}$ surface emission and the $4f^{12}$ bulk emission, which is tabulated in column 4 of Table III, increases with decreasing photon energy from 110 to 50 eV. This shows a decrease in the electron mean free path, when changing the photon energy from 110 to 50 eV.

The inset in Fig. 2 shows the Te $4d$ spectrum from a freshly cleaved TmTe(100) surface. In con-

trast to the Se $3d$ spectrum of TmSe(100), it is well described by a single spin-orbit-split doublet with no indication of a surface core-level shift. The fit with two Doniach-Šunjić-shaped lines results in a spin-orbit splitting of 1.47 ± 0.02 eV, which agrees rather well with a previous XPS measurement on crystalline Te.⁵⁰

C. TmS (100)

We have also studied surface effects on uv-photoemission spectra of a TmS(100) surface in the photon-energy range $30 \leq h\nu \leq 90$ eV. Some representative spectra obtained from the valence-band region are displayed in Figs. 3(a)–3(d). Bulk TmS is trivalent and metallic; accordingly the spectrum recorded at $h\nu = 30$ eV [Fig. 3(a)] reveals a high density of states of d -like conduction electrons at the Fermi level. Owing to the relatively small $4f$ -photoemission cross section⁴⁵ at this photon energy the spectrum is dominated by emission from the conduction band and the sulfur-derived valence band centered at 5.5 eV below E_F . At $h\nu = 50$ eV and higher, emission from Tm $4f$ states is dominating the spectra [Figs. 3(b)–3(d)], which clearly show multiplet structures from both $4f^{11}$ (Tm^{3+}) and $4f^{12}$ (Tm^{2+}) final states.

The emission from $4f^{12}$ final states originates from Tm atoms in the topmost surface layer of TmS(100), which is interpreted as due to a surface valence transition in the initial state of the Tm ions. The divalent Tm ions in the $4f^{13}(5d6s)^0$ initial state must be limited to the topmost surface layer of TmS(100), since a single $4f^{12}$ multiplet located at the Fermi level is sufficient to describe the experimental $4f^{12}$ spectral features [see Fig. 3(b)]. If TmS would be mixed valent in the bulk, or if the divalent Tm ions would extend over more than just the topmost surface layer, a superposition of two $4f^{12}$ final-state multiplets shifted by a surface core-level shift of similar magnitude as observed

TABLE III. Summary of results from the analysis of the TmTe spectra taken at four different photon energies: Δ_c is the surface core-level shift of the $4f^{12}$ multiplet, E_B is the binding energy of the bulk-multiplet component closest to E_F , R_1 is the ratio of integrated $4f^{12}$ surface to $4f^{12}$ bulk-multiplet intensities, l is the derived value for the mean free path. The error bars are given in parentheses in units of the last digits.

$h\nu$ (eV)	Δ_c (eV)	E_B^{12} (eV)	R_1	l (Å)
110	0.42 (6)	0.64 (5)	0.40 (6)	9.4 (12)
90	0.43 (7)	0.63 (5)	0.45 (6)	8.5 (11)
70	0.40 (6)	0.66 (5)	0.62 (8)	6.6 (8)
50	0.38 (6)	0.66 (5)	0.73 (10)	5.8 (8)

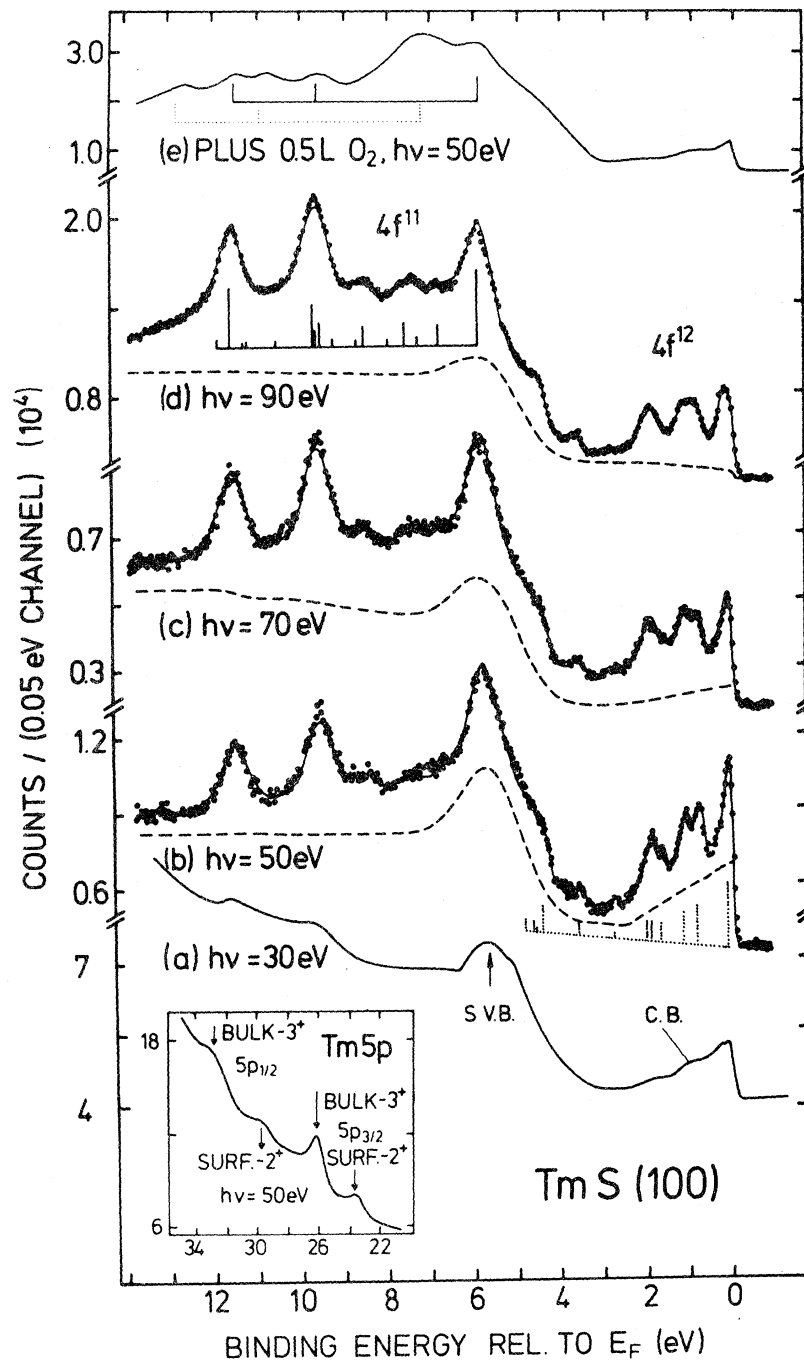


FIG. 3. Photoemission spectra of a freshly cleaved (100) surface of TmS excited with various photon energies. In the 30-eV spectrum the $4f$ features are very weak and emission from the d -like conduction band and the sulfur valence band is dominant. The solid lines in (b)–(d) represent the results of least-squares fits. The dashed lines represent the sum of the integral background and emission from the sulfur valence band and the conduction band. The bar diagrams represent the final-state $4f$ multiplets from the bulk (solid bars) and a surface layer (dotted bars).

for TmSe and TmTe would be expected. A further proof that the divalent Tm ions are limited to the topmost layer is given by the photon-energy dependence of the ratio R_2 of intensities of the $4f^{11}$ and

$4f^{12}$ spectral features (to be discussed below), and from the spectrum taken from a TmS(100) surface after exposure to 0.5 L of oxygen [Fig. 3(e)]. In the latter case, emission from $4f^{12}$ final states is

almost completely quenched, while—in addition to the $4f^{11}$ multiplet from bulk TmS—a further $4f^{11}$ multiplet shifted by 1.3 eV to higher binding energy is observed. As discussed in the TmSe and TmTe cases, this shifted multiplet originates from an insulating surface layer of trivalent $\text{Tm}_2\text{O}_3\text{S}$ produced by exposure to oxygen. The three most intense spectral features of each $4f^{11}$ final-state multiplet are indicated in Fig. 3(e) by solid (bulk TmS) and dotted (surface $\text{Tm}_2\text{O}_3\text{S}$) bar diagrams. The chemical shift between the two, which may be due to a reduced final-state screening in the insulating oxide surface layer, is very close to the one observed in the TmSe case.

This surface valence transition on TmS(100) is also observed via the Tm $5p$ photoemission spectrum shown in the inset of Fig. 3. Both the $5p_{1/2}$ and $5p_{3/2}$ final-state levels are split into two peaks, originating from trivalent bulk TmS and divalent surface TmS, respectively. The observed splitting is 2.6 ± 0.2 eV for the $5p_{3/2}$ line and 3.1 ± 0.4 eV for the $5p_{1/2}$ line. The difference may be due to an unresolved multiplet structure falsifying the true shifts. Both shifts are smaller than the one for adsorbate-covered TmTe,⁴⁷ where a binding-energy difference of 3.5 eV was determined by XPS measurements on the $5p_{3/2}$ levels of Tm^{3+} and Tm^{2+} .

The valence-band spectra of TmS(100) recorded at $h\nu=50, 70,$ and 90 eV were least-squares fitted with the same procedure described above for TmSe and TmTe. In this case, a triangular-shaped conduction band extending 2.5 eV below E_F , and a Gaussian of fixed width (1.60 eV FWHM) and fixed position (5.5 eV below E_F), describing emission from the sulfur-derived valence band, were added to the extrinsic background. The results of the fits are represented by the solid lines in Figs. 3(b)–3(d). As expected from the $h\nu$ dependences of partial cross sections,⁴⁵ the emission from the sulfur valence band and the conduction band strongly decreases from $h\nu=50$ eV to $h\nu=90$ eV.

In order to obtain optimum fits the intensities of two $4f^{12}$ -multiplet lines had to be slightly changed from the values used for the TmSe fits (Table I): 3F_4 was decreased to 1.77 and 3F_2 was decreased to 0.78. The same was true for three $4f^{11}$ -multiplet lines: ${}^4I_{15/2}$ was decreased to 2.3, ${}^4I_{13/2}$ was decreased to 0.50, and ${}^4I_{9/2}$ was increased to 0.70.

The fit results for three different photon energies are summarized in Table IV. Again a slightly reduced singularity index was obtained for the $4f^{12}$ surface lines, as compared to the $4f^{11}$ bulk multiplet. From the binding energies of the uppermost lines of the two multiplets listed in columns 2 and 3 of Table IV a mean value of 5.74 eV is obtained for the binding-energy difference. This is the smallest value in the series of the three compounds studied in this work. It is caused by the strong metallic screening of a bulk $4f^{11}$ hole in trivalent TmS, while the $4f^{12}$ hole is much less screened in the divalent surface layer. In column 4 of Table IV the ratio R_2 of the integrated intensity of the $4f^{12}$ surface multiplet to that of the $4f^{11}$ bulk multiplet is listed for the three photon energies. Owing to a decrease in the mean free path, R_2 increases from $h\nu=90$ eV to $h\nu=50$ eV.

IV. DISCUSSION

A. Bulk mean valence, surface-induced core-level shifts, and valence transition in TmSe

Stoichiometric TmSe is a well-known mixed-valent material which orders antiferromagnetically at $T_N \cong 3.46$ K.²⁹ As is known from systematic studies of lattice constants,^{28,30,51} of magnetic properties,³⁰ and of XPS spectra,³¹ the mean valence \bar{v} of Tm_xSe depends strongly on stoichiometry. For a stoichiometric sample with a lattice constant $a_0 = 5.71$ Å, as studied here, values of \bar{v} in the range from 2.77 to 2.55 have been obtained with

TABLE IV. Summary of results from the analysis of the TmS spectra at three photon energies: E_B is the binding energy of the multiplet component closest to E_F for the respective multiplet, R_2 is the ratio of integrated intensity of the $4f^{12}$ surface multiplet to that of the $4f^{11}$ bulk multiplet, l is the derived value for mean free path. Estimated error bars in units of the last digit are given in parentheses.

$h\nu$ (eV)	E_B^{12} (eV)	E_B^{11} (eV)	R_2	l (Å)
90	0.11 (3)	5.83 (4)	0.50 (7)	7.1 (10)
70	0.11 (3)	5.86 (4)	0.62 (9)	6.0 (8)
50	0.09 (3)	5.85 (4)	0.66 (10)	5.7 (8)

different methods. While lattice constant measurements give a mean valence near to 2.75, XPS (Ref. 31) and x-ray-absorption *L*-edge measurements^{33,34} arrive at values between 2.55 and 2.6. There are strong indications from magnetic³⁰ and Mössbauer²⁷ studies that TmSe is in a homogeneously mixed-valent state, even though x-ray-absorption and photoemission measurements cannot distinguish between homogeneously and inhomogeneously mixed-valent systems. The fact, however, that the uppermost multiplet line of the $4f^{12}$ bulk multiplet is found very close to the Fermi level (see Table II) is in favor of a homogeneously mixed-valent state.

In the XPS work of Ref. 31, the possibility of a surface valence transition in TmSe and its influence on the resulting value for \bar{v} was discussed. Such an effect could not be detected up to now in XPS measurements of a mixed-valent material due to limited resolution and reduced surface sensitivity. These factors should lead to a slightly smaller value for \bar{v} if not taken properly into account.³¹

In the present uv-photoemission studies of TmSe, the surface sensitivity is strongly enhanced, as compared to XPS measurements, due to much smaller mean free paths *l* for the emitted photoelectrons. The use of tunable synchrotron radiation, in addition, allows a variation of *l* and therefore of the surface sensitivity. The increase in the surface sensitivity due to a decrease in the electron mean free path *l*, when changing the photon energy from 100 to 45 eV, is clearly visible in the spectra of Fig. 1, manifesting itself in an increase of the relative intensity of the $4f^{12}$ surface multiplet (represented by the dotted bar diagram).

A surface valence transition in a mixed-valent material was recently characterized for the first time on the surface of a single crystal of YbAl₂,¹⁰ and it was shown that the thickness of a divalent surface layer extends over more than one atomic layer in this case. It was argued that the large magnitude of surface core-level shifts observed for YbAl₂ ($\Delta_{c1}=0.92$ eV for the topmost and $\Delta_{c2}\cong 0.35$ eV for an underlying surface layer) is obviously sufficient to stabilize the divalent state even in a "second" layer of this mixed-valent material.

In the present case of TmSe(100), the photoemission spectra of Fig. 1 also show a dominant emission from $4f^{12}$ (Tm²⁺) multiplets, an observation that is only in accord with a mean bulk valence in the range from 2.5 to 2.75 if the topmost surface layer is in the divalent state. If no surface valence transition were taken into account, a value of

$\bar{v}=2.36$ would be obtained from the fractional intensities $I^{12}=I_B^{12}+I_S^{12}$, and I^{11} , listed in Table II, with the use of the relation

$$\bar{v}=2+I^{11}/(I^{11}+12I^{12}/13).$$

Here, the intensities were normalized to the same number of $4f$ electrons in the initial state (12 and 13, respectively, for Tm³⁺ and Tm²⁺). Quite clearly, this value cannot be reconciled with the values for \bar{v} obtained by other measurements, which means that also in TmSe a surface layer of thickness Δs is in the divalent state.

To obtain an estimate for the thickness Δs of the divalent surface layer of TmSe we use the equation

$$\begin{aligned} I_S/I_B &= I_S^{12}/(I_B^{12}+13I^{11}/12) \\ &= \exp(\Delta s/l) - 1, \end{aligned} \quad (1)$$

where equal photoemission cross sections were assumed for surface and bulk Tm atoms, and the observed intensities were again normalized to the same number of $4f$ electrons in the initial state. With the fractional intensities in Table II, we arrive at $\Delta s/l=0.41$ and 0.45 for $h\nu=100$ and 70 eV, respectively. With an estimate of $l\cong 6$ Å for electrons of about 60-eV kinetic energy,¹⁰ the value of $\Delta s/l=0.46$ obtained from the 70-eV spectrum results in $\Delta s\cong 2.76$ Å, which is very close to the thickness of the topmost surface layer ($a_0/2=2.855$ Å) of the (100) surface of TmSe. We thus arrive at the conclusion that just one surface layer of TmSe(100) is divalent. This finding is actually plausible in view of the smallness of the surface core-level shift, $\Delta_c=0.32\pm 0.04$ eV, observed for the topmost surface layer. From the experimental findings in YbAl₂ and from theoretical considerations,⁵² the shift in binding energy of the second surface layer is expected to be a factor of $\cong 3$ smaller than the one for the topmost layer, which would amount to only about 0.1 eV in the case of TmSe(100). Such a small stabilization of the $4f$ level in the second layer may not be sufficient to cause a valence transition in the second surface layer. We believe, however, that surface valence transitions in at least one surface layer are always present in mixed-valent materials. All mixed-valent systems in addition to TmSe studied so far in detail, namely YbAl₂,¹⁰ EuPd₂Si₂,¹² and Sm_{1-x}Y_xS,¹¹ exhibit such effects.

Since the present photoemission spectra—due to the surface core-level shifts—allow a separation of the emitted $4f^{12}$ intensities from the topmost surface layer (I_S^{12}) and the bulk (I_B^{12} from second and

deeper layers), a determination of the mean bulk valence \bar{v} is, in principle, possible with the use of the fractional intensities of Table II and the following equation:

$$\bar{v} = 2 + I^{11} / (I^{11} + 12I_B^{12} / 13) . \quad (2)$$

In this way we arrive at values for \bar{v} of 2.56 (2.53) from the intensities determined from the 100-eV (70-eV) spectrum. We adopt a value of $\bar{v} = 2.55 \pm 0.05$ for the mean bulk valence of TmSe. This value is again smaller than the estimates from the lattice constant of TmSe,^{28,30} but fits rather well in the range of values determined with other methods (XPS, x-ray-absorption *L*-edge spectroscopy, and magnetic measurements). It is interesting to note that the XPS results of Ref. 31, uncorrected for a divalent surface layer, did not result in a smaller value for \bar{v} than the present measurements. Taking into account the strongly reduced surface sensitivity of the XPS measurements (by about a factor of 5 as compared to $h\nu \cong 70$ eV) the surface-uncorrected XPS results for \bar{v} should be too small by about 0.05. Even though this small discrepancy cannot be clarified here, we would like to mention several factors which may give erroneous values for \bar{v} in a photoemission experiment: (i) The surfaces of rare-earth materials are extremely reactive to oxygen contamination, causing in most mixed-valent materials the intensity of the trivalent multiplets to increase with time.^{47,48} Such a surface oxidation would result in \bar{v} values too large for a mixed-valent material. (ii) Even with ideally clean surfaces, final-state effects, which have been identified in deep-core-level spectra of rare earths^{53,49} and which have not been ruled out for *4f* spectra,^{20,54} may falsify the resulting \bar{v} values.

The splitting of the Se *3d* levels in TmSe(100) into two doublets separated by 0.52 ± 0.05 eV must be interpreted as due to a surface effect on the Se *3d* binding energy. It is not primarily related to the mixed-valent character of TmSe, since an identical splitting of the Se *3d* levels has also been observed in highly diluted $\text{Tm}_{0.01}\text{Y}_{0.99}\text{Se}$,⁵⁵ where most of the Se atoms have Y neighbors. On the basis of the photon-energy dependence of the intensity ratio of the two doublets and the spectrum obtained from a TmSe surface exposed to 1.5 L of O₂, the spin-orbit-split *3d* doublet at lower binding energy is interpreted as the surface doublet. Surface core-level shifts of similar magnitude and sign have recently also been observed for the anion core levels of uranium chalcogenides.⁵⁶

B. Surface core-level shift in TmTe(100)

TmTe is a divalent semiconductor with a lattice constant of 6.43 Å, which corresponds closely to the pure divalent state.²⁶ Even though early XPS studies claimed that TmTe is a mixed-valent material,⁴⁷ later optical-absorption and uv-photoemission studies showed the absence of Tm³⁺ in TmTe as well as a high sensitivity of the TmTe surface to oxygen contamination.⁴⁸ The present spectra support the divalent state of TmTe, since the uppermost *4f*¹²-multiplet line is 0.65 eV below *E_F*, which clearly shows that *4f*¹³ and *4f*¹²(*5d 6s*)¹ are not degenerate in the initial state. The weak intensity of the *4f*¹¹ final-state multiplet, visible in Fig. 2(a), which amounts to less than 5% of the *4f*¹² intensity, must then be interpreted as either due to oxygen contamination of the surface or due to a two-hole final state (*4f* shake-up process).^{49,54,20}

No surface-induced core-level shift could be resolved for the *4d* level of Te, in contrast to the Se *3d* case in TmSe. This may partly be due to smaller Te *4d* shifts as expected from the absence of metallic screening in TmTe.

C. Surface valence transition in TmS

The lattice constant of trivalent metallic TmS ($a_0 = 5.42$ Å) fits well in the systematic variation of lattice constants of other trivalent rare-earth sulfides.²⁶ TmS orders antiferromagnetically at $T_N = 5.2$ K, exhibiting an effective magnetic moment close to the Tm³⁺ value.²⁶ A previous XPS study of TmS confirmed its trivalent nature in the bulk.⁵⁷

Valence changes at the surface of bulk trivalent rare-earth solids had previously been observed for Sm metal⁵ and for the intermetallic compound YbAu₂.⁷ The divalent *4f*¹² final-state multiplet in the spectra of TmS, reported here, represent the first observation of the valence change at the surface of a Tm compound. Johansson has argued¹ on the basis of thermochemical arguments that Tm metal should not undergo a valence transition at the surface, in agreement with experimental observation.^{25,58} As was argued above, the present results confirm the bulk trivalent nature of TmS, since the divalent *4f*¹² final-state multiplet observed is not split into two multiplets, i.e., it must originate completely from Tm atoms in the top-most surface layer of Tm.

D. Electron mean free path l

The present results may be used to derive absolute values for the electron mean free path l as a function of photon energy, if we assume that the thickness of the topmost surface layer is equal to half the lattice constant in each case (TmSe, TmTe, TmS). This follows directly from the NaCl structure of the (100) surfaces studied, if the effects of a possible surface relaxation are neglected. In addition, we have to assume that just the topmost (100)-surface layers are involved in the observed surface valence transitions (TmSe, TmS) or surface-shifted $4f^{12}$ multiplets (TmSe, TmTe). As discussed above, this latter assumption is strongly supported by the experimental observations in each case.

In a continuum model, where we assume the intensity of photoelectrons emitted normal to the surface from a layer at distance x from the surface to be proportional to $\exp(-x/l)$, we arrive at the following expression for the mean free path l :

$$l = \Delta s / \ln(1 + R) . \quad (3)$$

Here R represents the ratio of emitted $4f$ intensity from the surface layer of thickness Δs to that emitted from all deeper layers together, with the $4f$ intensities being normalized to the same number of $4f$ electrons in the initial states (12 for Tm^{3+} and 13 for Tm^{2+}). To derive Eq. 3, we have assumed equal photoemission cross sections for surface and bulk layers, and we have neglected a small geometrical correction due to electron emission into a 35° cone normal to the surface ($\cos\theta \cong 1$) in the present experimental arrangement.

For the three Tm-chalcogenide surfaces investigated the ratios R are then given by the following expressions of the fractional intensities listed in Tables II, III, and IV:

$$\begin{aligned} R &= I_S^{12} / (I_B^{12} + 13I^{11}/12) \quad \text{for TmSe} , \\ R &= R_1 = I_S^{12} / I_B^{12} \quad \text{for TmTe} , \\ R &= 12R_2/13 = 12I_S^{12} / 13I_B^{11} \quad \text{for TmS} . \end{aligned} \quad (4)$$

The resulting values for the electron mean free path l are plotted in Fig. 4 as a function of the kinetic energy of the photoelectrons above E_F for the three Tm compounds studied. The abscissa values of Fig. 4 represent the average kinetic energy of the photoelectrons employed in deriving a specific l value. In all three cases l decreases with decreasing kinetic energy even below 50 eV. No minimum in l is observed in the studied energy range in contrast to the so-called "universal curve"

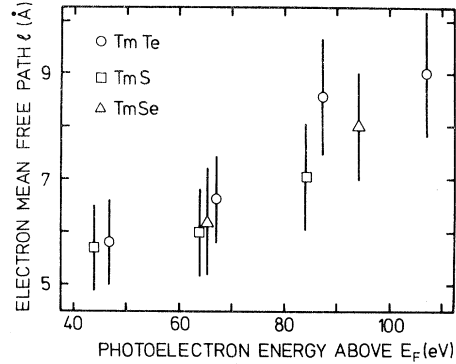


FIG. 4. Electron mean free path l as a function of kinetic energy of the photoelectrons above E_F for TmS, TmSe, and TmTe.

for the energy dependence of l .^{59,60} A quite similar behavior of l has recently also been observed for several of the rare-earth metals,²¹ where increasing surface sensitivity down to electron energies of 30 eV was found. Despite the large error bars, the l values for the metals TmS and TmSe seem to be systematically smaller than those for the semiconductor TmTe. This could be due to additional loss processes caused by interaction of the photoelectrons with conduction electrons. For a more quantitative discussion, data of higher accuracy are needed.

E. Final-state multiplets and line shapes

In the least-squares-fit analysis of the final-state Tm multiplets we have observed deviations of the fitted intensities of some multiplet lines from the calculated ones, even in those cases where the original LS -coupling calculations³⁵ had been improved by intermediate-coupling calculations.^{36,41} Such deviations of the $4f^{11}$ -line intensities have also been observed in high-resolution XPS spectra of Tm metal.⁶¹ Quite similar as in the present measurements, the $^4I_{9/2}$ line had higher intensity, while the $^4F_{9/2}$, $^2H_{11/2}$, $^2D_{5/2}$, and $^4D_{7/2}$ lines were observed with smaller intensities than predicted theoretically. The spectra of Tm metal presented in Ref. 25 seem to indicate a photon-energy dependence, while the present experiments reveal certain solid-state effects on the intensities of some multiplet lines. As described above, slightly different sets of intensities had to be used for the three solids in order to obtain optimum least-squares fits.

In contrast to the line intensities we do not observe, within the present experimental accuracy,

differences in the splittings of the $4f^{11}$ and $4f^{12}$ multiplets for the three compounds studied. The splitting of the $4f^{12}$ multiplet was taken directly from the results of uv-absorption measurements of Tm^{3+} , while the splitting of the $4f^{11}$ multiplet had to be assumed 11% larger than the one of Er^{3+} in all three cases. This is somewhat at variance with a statement made in Ref. 19 concerning the case of Eu metal, where a scaling factor of 0.93 was used for the splitting of the $\text{Eu}^{2+}4f^6$ final-state multiplet as compared to the uv-photoabsorption results for Eu^{3+} . These still open questions concerning intensities and positions of individual multiplet lines should be studied with high accuracy on well-split final-state $4f$ multiplets such as, e.g., those of Tm systems.

The Doniach-Šunjić line shapes⁴³ used in the present least-squares-fit analysis are based on the assumption of a structureless density of final states above E_F . It has been shown previously that in cases of only moderately asymmetric lines the line shapes obtained from specific final-state densities deviate only slightly from Doniach-Šunjić profiles, the main difference being in the convergence behavior of the energy-loss tails.⁶² Therefore, in view of the small asymmetry parameters α of the present spectra the Doniach-Šunjić line-shape analysis appears to be a reasonable approximation.

For all three compounds the least-squares fits resulted in systematically smaller singularity indices α for the surface multiplets ($\alpha_S \cong 0.10$) as compared to the bulk multiplets ($\alpha_B \cong 0.17$). This is in agreement with the observation that the topmost surface layers are divalent in all three compounds studied, which reduces the probability for intrinsic energy losses due to excitations of conduction electrons.⁴³ In addition, a smaller probability for external losses was also observed for photoelectrons from the topmost surface layer, expressing itself in a smaller integral background as compared to the one caused by photoelectrons from the bulk.

V. CONCLUSIONS

The unique series of rare-earth monochalcogenides, divalent TmTe, trivalent TmS, and mixed-valent TmSe were studied by high-resolution photoemission spectroscopy in the photon-energy range $30 \leq h\nu \leq 110$ eV.

On vacuum-cleaved (100) surfaces, a shift of the Tm $4f$ levels of 0.32 ± 0.04 eV (0.41 ± 0.05) to higher binding energy was observed for the top-

most surface layer of TmSe (TmTe). The topmost surface layer of mixed-valent TmSe was found to be in the divalent state. A surface-induced valence transition to the divalent state was also observed for the topmost surface layer of TmS(100). No surface core-level shift of the $4f$ levels can therefore be determined for TmS, since the $4f^{12}$ spectral feature originates completely from the surface, while the $4f^{11}$ intensity originates altogether from the bulk. From an analysis of the fractional intensities of the $4f^{12}$ final-state multiplets originating from the topmost surface layer and the bulk, as well as of the $4f^{11}$ final-state multiplet from the bulk, a value of $\bar{v} = 2.55 \pm 0.05$ could be derived for the bulk mean valence of TmSe. In all three cases the surface-induced divalent spectral features could be removed from the spectra by exposing the surfaces to 0.5 to 1.5 L of oxygen. This resulted in a trivalent surface layer in all three cases, probably a $\text{Tm}_2\text{O}_2\text{X}$ compound (with $X = \text{S, Se, Te}$), manifesting itself in an intense $4f^{11}$ multiplet at higher binding energy than those originating from bulk TmSe and TmS, respectively. A surface core-level shift of 0.52 ± 0.05 to lower binding energy was also observed for the $3d$ levels of Se atoms located in the topmost surface layer of TmSe(100). No shift of the Te $4d$ levels, however, could be resolved for TmTe. Reduced intrinsic and extrinsic losses were found for the topmost, divalent surface layers, manifesting themselves in reduced singularity indices α and reduced integral backgrounds as compared to the bulk. Absolute values for the electron mean free path l were derived from the data, which decrease with decreasing kinetic energy of the photoelectrons down to $\cong 44$ eV.

ACKNOWLEDGMENTS

The authors would like to thank Professor P. A. Cox for making available unpublished results of intermediate-coupling calculations for $4f^{11}$ -multiplet intensities. Fruitful discussions with F. J. Himpsel and W. D. Schneider as well as the support by J. J. Donelon, A. Marx, and the staff of the Synchrotron-Radiation Center of the University of Wisconsin are gratefully acknowledged. The work was partly supported by the Air Force Office of Scientific Research under Contract No. F-49620-81-C0089 and the Bundesministerium für Forschung und Technologie under Contract No. 05 127 KA.

- ¹B. Johansson, *Phys. Rev. B* **19**, 6615 (1979).
- ²B. Johansson and N. Mårtensson, *Phys. Rev. B* **21**, 4427 (1980).
- ³A. Rosengren and B. Johansson, *Phys. Rev. B* **23**, 3582 (1981).
- ⁴G. Wertheim and M. Campagna, *Chem. Phys. Lett.* **47**, 182 (1977).
- ⁵G. K. Wertheim and G. Crecelius, *Phys. Rev. Lett.* **40**, 813 (1978).
- ⁶J. W. Allen, L. I. Johansson, R. S. Bauer, I. Lindau, and S. B. M. Hagström, *Phys. Rev. Lett.* **41**, 1499 (1978).
- ⁷G. K. Wertheim, J. H. Wernick, and G. Crecelius, *Phys. Rev. B* **18**, 875 (1978).
- ⁸G. Crecelius and G. K. Wertheim, *J. Magn. Magn. Mater.* **15-18**, 1074 (1980).
- ⁹G. Krill, J. Durand, A. Berrada, N. Hassanain, and M. F. Ravet, *Solid State Commun.* **35**, 547 (1980).
- ¹⁰G. Kaindl, B. Reihl, D. E. Eastman, R. A. Pollak, N. Mårtensson, B. Barbara, T. Penney, and T. S. Plaskett, *Solid State Commun.* **41**, 157 (1982).
- ¹¹B. Reihl, F. Holtzberg, G. Hollinger, G. Kaindl, N. Mårtensson, and R. A. Pollak, in *Valence Instabilities*, edited by P. Wachter (North-Holland, Amsterdam, in press).
- ¹²N. Mårtensson, B. Reihl, W. D. Schneider, V. Murgai, L. C. Gupta, and R. D. Parks, *Phys. Rev. B* **25**, 1446 (1982).
- ¹³P. H. Citrin, G. K. Wertheim, and Y. Baer, *Phys. Rev. Lett.* **44**, 1425 (1978).
- ¹⁴Tran Minh Duc, C. Guillot, Y. Lassailly, J. Lecante, Y. Jugnet, and J. C. Vedrine, *Phys. Rev. Lett.* **43**, 789 (1979).
- ¹⁵J. F. Van der Veen, F. H. Himpsel, and D. E. Eastman, *Phys. Rev. Lett.* **44**, 189 (1980).
- ¹⁶S. F. Alvarado, M. Campagna, and W. Gudat, *J. Electron Spectrosc. Relat. Phenom.* **18**, 43 (1980).
- ¹⁷J. K. Lang and Y. Baer, *Solid State Commun.* **24**, 253 (1977).
- ¹⁸J. W. Allen, L. I. Johansson, I. Lindau, and S. B. Hagström, *Phys. Rev. B* **21**, 1335 (1980).
- ¹⁹R. Kammerer, J. Barth, F. Gerken, A. Flodström, and L. I. Johansson, *Solid State Commun.* **41**, 435 (1982).
- ²⁰W. D. Schneider, C. Laubschat, G. Kaindl, B. Reihl, and N. Mårtensson, in *Valence Instabilities*, edited by P. Wachter (North-Holland, Amsterdam, in press).
- ²¹F. Gerken, J. Barth, R. Kammerer, L. I. Johansson, and A. Flodström, *Surf. Sci.* (in press).
- ²²W. Gudat, M. Campagna, R. Rosei, J. H. Weaver, W. Eberhardt, F. Hullinger, and E. Kaldis, *J. Appl. Phys.* **52**, 2123 (1981).
- ²³N. Mårtensson, B. Reihl, R. A. Pollak, F. Holtzberg, and G. Kaindl, *Phys. Rev. B* **25**, 6522 (1982).
- ²⁴G. Kaindl, W. D. Schneider, B. Reihl, G. Hollinger, and N. Mårtensson (unpublished).
- ²⁵L. I. Johansson, J. W. Allen, and I. Lindau, *Phys. Lett.* **86A**, 442 (1981).
- ²⁶E. Bucher, K. Andres, F. J. di Salvo, J. P. Maita, A. C. Gossard, A. S. Cooper, and G. W. Hull, Jr., *Phys. Rev. B* **11**, 500 (1975).
- ²⁷B. B. Triplett, N. S. Dixon, P. Boolchand, and S. S. Hanna, *J. Phys. Paris Colloq.* **35**, C6-653 (1974).
- ²⁸B. Batlogg, H. R. Ott, E. Kaldis, W. Thöni, and P. Wachter, *Phys. Rev. B* **19**, 247 (1979).
- ²⁹P. Haen, F. Lapierre, J. M. Mignot, A. Tournier, and F. Holtzberg, *Phys. Rev. Lett.* **43**, 304 (1979).
- ³⁰F. Holtzberg, T. Penney, and R. Tournier, *J. Phys. Paris Colloq.* **40**, C5-314 (1979).
- ³¹G. K. Wertheim, W. Eib, E. Kaldis, and M. Campagna, *Phys. Rev. B* **22**, 6240 (1980).
- ³²B. Batlogg, E. Kaldis, and H. R. Ott, *Phys. Lett.* **62A**, 270 (1977).
- ³³H. Launois, M. Rawiso, E. Holland-Moritz, R. Pott, and D. Wohlleben, *Phys. Rev. Lett.* **44**, 1271 (1980).
- ³⁴A. Bianconi, S. Modesti, M. Campagna, K. Fischer, and S. Stizza, *J. Phys. C* **14**, 4737 (1981).
- ³⁵P. A. Cox, in *Structure and Bonding*, edited by J. D. Dunitz *et al.* (Springer, Berlin, 1975), Vol. 24, p. 59.
- ³⁶N. Beatham, P. A. Cox, A. F. Orchard, and I. P. Grant, *Chem. Phys. Lett.* **63**, 69 (1979).
- ³⁷D. E. Eastman, J. J. Donelon, N. C. Hien, and F. J. Himpsel, *Nucl. Instrum. Methods* **172**, 327 (1980).
- ³⁸F. Holtzberg, F. von Molnar, and J. M. D. Coey, in *Handbook on Semiconductors*, edited by F. P. Keller (North-Holland, Amsterdam, 1980), Vol. 3, p. 803.
- ³⁹J. F. Herbst, R. E. Watson, and J. W. Wilkins, *Phys. Rev. B* **17**, 3089 (1978).
- ⁴⁰W. T. Carnall, P. R. Fields, and K. Rajnak, *J. Chem. Phys.* **49**, 4424 (1968).
- ⁴¹P. A. Cox and J. K. Lang (unpublished); J. K. Lang, Ph.D. Thesis, Eidgenössische Technische Hochschule, Zürich, 1979 (unpublished).
- ⁴²See, e.g., J. Flahaut, in *Handbook of the Physics and Chemistry of Rare Earths*, edited by K. A. Gschneidner, Jr. and LeRoy Eyring (North-Holland, Amsterdam, 1979), Vol. 4, p. 1.
- ⁴³S. Doniach and M. Sunjic, *J. Phys. C* **3**, 285 (1970).
- ⁴⁴M. Campagna, J. E. Rowe, S. B. Christman, and E. Bucher, *Solid State Commun.* **25**, 249 (1978).
- ⁴⁵S. M. Goldberg, C. S. Fadley, and S. Kono, *J. Electron Spectrosc. Relat. Phenom.* **21**, 285 (1981).
- ⁴⁶N. J. Shevchik, M. Cardona, and J. Tejada, *Phys. Rev. B* **8**, 2833 (1973).
- ⁴⁷M. Campagna, E. Bucher, G. K. Wertheim, and D. N. E. Longinotti, *Phys. Rev. Lett.* **32**, 885 (1974).
- ⁴⁸R. Suryamarayanan, G. Güntherodt, J. L. Freeouf, and F. Holtzberg, *Phys. Rev. B* **12**, 4215 (1975).
- ⁴⁹W. D. Schneider, C. Laubschat, I. Nowik, and G. Kaindl, *Phys. Rev. B* **24**, 5422 (1981).
- ⁵⁰R. A. Pollak, S. P. Kowalczyk, L. Ley, and D. A. Shirley, *Phys. Rev. Lett.* **29**, 274 (1972).
- ⁵¹E. Kaldis, B. Fritzler, and W. Peterler, *J. Magn. Magn. Mater.* **15-18**, 985 (1980).
- ⁵²D. Tománek, V. Kumar, S. Holloway, and K. H. Bennemann, *Solid State Commun.* **41**, 273 (1982).
- ⁵³J. C. Fuggle, M. Campagna, Z. Zolnierrek, R. Lässer,

- and A. Platau, Phys. Rev. Lett. 45, 1597 (1980).
- ⁵⁴B. Johansson and N. Mårtensson, Phys. Rev. B 24, 4484 (1981).
- ⁵⁵N. Mårtensson, B. Reihl, R. A. Pollak, F. Holtzberg, G. Kaindl, and D. E. Eastman, Phys. Rev. B 26, 648 (1982).
- ⁵⁶N. Mårtensson, B. Reil, and U. Vogt, Phys. Rev. B 25, 824 (1982).
- ⁵⁷M. Campagna and G. K. Wertheim, in *Structure and Bonding* edited by J. D. Dunitz *et al.* (Springer, Berlin, 1976), Vol. 30, p. 99.
- ⁵⁸Y. Baer and G. Busch, J. Electron Spectrosc. Relat. Phenom. 5, 611 (1974), and references therein.
- ⁵⁹I. Lindau and W. E. Spicer, J. Electron Spectrosc. Relat. Phenom. 3, 409 (1974).
- ⁶⁰J. Szajman, J. Liesegang, J. G. Jenkin, and R. C. G. Leckey, J. Electron Spectrosc. Relat. Phenom. 23, 97 (1981); and references therein.
- ⁶¹J. K. Lang, Y. Baer, and P. A. Cox, J. Phys. F 11, 121 (1981).
- ⁶²G. K. Wertheim, Phys. Rev. B 25, 1987 (1982), and references therein.